

# We are IntechOpen, the world's leading publisher of Open Access books Built by scientists, for scientists

6,900

Open access books available

185,000

International authors and editors

200M

Downloads

Our authors are among the

154

Countries delivered to

TOP 1%

most cited scientists

12.2%

Contributors from top 500 universities



WEB OF SCIENCE™

Selection of our books indexed in the Book Citation Index  
in Web of Science™ Core Collection (BKCI)

Interested in publishing with us?  
Contact [book.department@intechopen.com](mailto:book.department@intechopen.com)

Numbers displayed above are based on latest data collected.  
For more information visit [www.intechopen.com](http://www.intechopen.com)



# Resonance Raman Spectroscopy Investigation of the Interaction of Molecules Adsorbed on Solid Acid Surfaces

*Lucia Kiyomi Noda*

## Abstract

Many solid acids with very strong acid sites, as some zeolites, transition metal exchanged montmorillonites, sulfated metallic oxides, are known to have the oxidizing ability, which can be related to the catalytic activity of these materials. The interaction of these solid acids with aromatic molecules can give rise to several oxidation products. Intermediate species of aromatic molecules formed by interaction with strong solid acids had been reported, as radical cations, proving the oxidizing ability of the solids. Besides radical cations, charge transfer complexes between the solid acids and aromatic molecules can be formed. These radical cations and charge transfer complexes usually show absorption bands in the visible region, opening the possibility of studying these species by Resonance Raman Spectroscopy (RRS). Benzene and substituted benzenes, phenothiazine, t-stilbene, adsorbed on solid acids, are examples of molecules that had been investigated by RRS. Exciting the spectrum with suitable radiation makes it possible to observe the RRS of the species of interest even when its concentration is low, because of the preferential enhancement of the vibrational modes of the chromophore. A review of RRS studies of molecules adsorbed on solid acids is presented. RRS proved valuable in characterizing intermediate species as radical cations or charge transfer complexes formed on the solid acids.

**Keywords:** resonance Raman spectroscopy, solid acids, radical cation, charge transfer complex

## 1. Introduction

Solid acids are the most important solid catalysts nowadays, considering not only the total amount used but also the final economic impact. Solid catalysts have a great advantage over liquid catalysts. They are, in fact, generally almost fully recovered from reaction products without any operation or with quite easy procedures.

Probably infrared spectroscopy is the most largely used spectroscopy technique to study the adsorption of molecules on solid surfaces. Other techniques need an ultra-high vacuum, while IR spectroscopy can be investigated over a wide range of temperatures and pressures. However, most of the materials used as adsorbents, for instance, semiconductor and insulator surfaces, have strong IR signals, so the spectrum is predominantly that of the adsorbent, which is a disadvantage [1].

Compared to infrared absorption spectroscopy, Raman scattering has an inherently low sensitivity. But this limitation was largely surpassed by the development of high-performance single-stage spectrometers combined with notch filters and CCD cameras. Moreover, the sensitivity of Raman spectroscopy can be increased by taking advantage of resonance effects, for example in resonance Raman spectroscopy, coherent anti-Stokes Raman spectroscopy (CARS), surface-enhanced Raman spectroscopy (SERS), or tip-enhanced Raman spectroscopy (TERS) [2].

The interaction of molecules adsorbed on solid acids can be weak or strong, but in solids with higher acidity, the interaction is often so strong that electron abstraction may occur, occurring in fact a redox reaction. It depends not only on the acidity of the solid acid but also on the ionization potential of the adsorbed molecule. Organic molecules with relatively low ionization potential can be ionized giving rise to radical cations. However, depending on some conditions, a charge transfer complex is observed. Radical cations of molecules with extended conjugation, as polyenes and some aromatic molecules, have electronic absorption shifted to the visible region of the spectrum, opening the possibility of exploring the Resonance Raman effect with the enhancement of the chromophore responsible for the electronic transition.

The theory behind the resonance Raman Effect will not be presented here, but for whoever is interested, the excellent article by Clark and Dines is recommended [3].

In the present review the interaction of organic molecules with high acidity solids and the species resulting from the interaction, observed through Resonance Raman spectroscopy (RRS), is presented. Three types of solid acids, zeolites, clays, and sulfated metallic oxides, are chosen because of the greater number of RRS studies with these solid acids.

## 2. Zeolites

Zeolites are crystalline aluminosilicates with general chemical composition  $M_{x/n}^{x+}[Al_xSi_yO_{2(x+y)}]zH_2O$ . Its lattice consists of a network of  $SiO_4^{4-}$  and  $AlO_4^{4-}$  tetrahedra with Si or Al atoms at the centers and oxygen atoms in each corner. The presence of aluminum atoms replacing silicon atoms in the zeolite network creates an excess negative charge. Charge-compensating cations ( $M^+$ ) are introduced into the structure to compensate for the negative charge. These readily exchangeable cations are not covalently bound to the zeolite framework [4].

The Si/Al ratio may vary from Si/Al = 1 (faujasite X) to Si/Al =  $\infty$  (silicalite). The number of cations in the framework and the zeolite properties as the thermal and chemical stability or the polarity of the internal surfaces are determined by the Al content.

Electron transfer processes at interfaces are central to many important chemical processes and are vital to energy conversion and storage technologies. Investigations of the mechanism of electron transfer reactions at interfaces are often difficult to perform because of the heterogeneity of the surfaces and because the reaction intermediates, often radicals, are generally highly reactive and difficult to isolate for extended periods of time to allow detailed characterization [5].

A common way to stabilize these intermediates is their isolation in frozen rare gas or halocarbon matrices.

Zeolites and other porous solids are an alternative to the study of electron-transfer processes, allowing the stabilization of radical cations for longer periods of time [6]. Garcia and Roth had made an extensive review about the generation and reaction of organic radical cation in zeolites [7].

Some acid zeolites have the ability to generate spontaneously organic radical cations upon adsorption of organic electron donors or the radical cations can be

generated by the action of radiation or light. The restricted mobility within zeolite pores limits the tendency of free radicals or radical cations to dimerize and prevents access to reagents that typically would cause their decay in solution.

The spontaneous ionization depends on the ionization potential of the guest as well as on the ionizing capacity of the host, which is directly related to the Si/Al ratio and to the nature of the charge balancing cation. The highest yield was found from  $H^+$ . Ramamurthy et al. showed that an increasing Al content enhanced the electron acceptor ability [4]. They reported the generation of stable radical cations from  $\alpha,\omega$ -diphenyl polyenes (trans-stilbene, trans, trans-1,4-diphenyl butadiene, all-trans-1,6-diphenylhexatriene, and all-trans-1,8-diphenyl-1,3,5,7-octatetraene upon inclusion in the channels of pentasil zeolites.

A systematic spectroscopic investigation of radical species of several organic molecules formed upon the interaction with zeolites was done by Moissette in the 2000s and 2010s. Most of the investigated molecules are aromatic, as trans-stilbene anthracene and other ones. UV-visible, ESR, and Raman spectra were obtained with excitation in and off-resonance, but in the present review, only the resonance Raman results of Moissette are presented. Only the Moissette results with t-stilbene and N, N, N', N'-tetramethyl-p-phenylenediamine (TMPD) and N, N, N', N'-tetramethylbenzidine (TMB) are included in this review, but Moissette investigated a larger number of molecules, as can be found in the literature.

## 2.1 Trans-stilbene

Many Moissette studies were done with trans-stilbene, a molecule considered as a prototype system for the photoisomerization reaction and as a model for photosensitized electron-donor structure [8]. Trans-Stilbene (E-1,2-diphenylethene, t-St) has a relatively low ionization potential value ( $I_g = 7.65$  eV in the gas phase) and has the appropriate dimensions to enter the channels of medium-pore zeolites [9]. Moissette et al. investigated the formation of t-stilbene radicals in HZSM-5 and HFER zeolites, that differ in their pore size [10]. As HFER has a narrower pore size the radical cation is the only stable species while in the larger pore diameter HZSM-5, the electron transfers are faster and the radical cation (RC) evolves after several minutes/hours to a charge transfer complex (CTC). Three exciting laser lines, at 473, 515, and 633 nm, have been used to take advantage of the RR effect. The wavelengths have been chosen to correspond to the absorptions of the charge separated states and could give rise to resonance Raman enhancement of the specific vibrational modes of the radical cation or the charge transfer complex. The RC has a characteristic band at 475 nm, while the bands at 565 and 625 nm are characteristic of CTC 1 and the bands at 375 and 700 nm are characteristic of CTC 2. Exciting with 473 nm Raman bands at 1285 and 1605  $cm^{-1}$  and a weak band at about 1565  $cm^{-1}$  were observed. The spectrum excited with 515 nm presents the same main Raman bands characteristic of RC at 1290 and 1609  $cm^{-1}$  as well as the contributions at 1560 and 1550  $cm^{-1}$ . The resonance effect of the RC species is not as marked as at 473 nm given that the excitation is in the lower energy side of the absorption band. A broadening is observed especially at about 1600  $cm^{-1}$  corresponding to the position of CTC contribution. Exciting with 633 nm broad and intense bands centered at 1596  $cm^{-1}$  and 1192  $cm^{-1}$  containing several contributions are observed. Several bands of lower intensity are also observed around 1320  $cm^{-1}$ . These features were assigned to the resonance-enhanced bands of the CTC 1 species. The authors do not assign Raman bands to CTC 2 species, but the broadening of the Raman bands exciting with 633 nm may be a sign of the presence of another species.

When t-St was adsorbed in the medium size channel of nonacidic NaZSM-5 zeolite, the interaction between  $Na^+$  cation and t-St occurred through one phenyl group coordinated to the  $Na^+$  cation [11]. The similarity between Raman spectra of t-St in



solution and occluded in NaZSM-5 led the authors to conclude that the interaction was weak, with no radical formation. Only with laser UV (266 nm) photoionization  $t\text{-St}^{*+}$  was generated. Exciting with 4880 nm resonance Raman bands of the radical cation was observed. With 632 nm excitation, a different spectrum was observed, assigned to a primary  $t\text{-St}^{*+}$ -electron pair. Contrary to Moissette that did not observe spontaneous ionization of  $t$ -stilbene in NaZSM-5 zeolite, Ramamurthy [4] reported the formation of radical cation species upon adsorption of  $t$ -stilbene on the zeolite. Ramamurthy made the adsorption of  $t$ -stilbene diluted in a trimethylpentane solution. As Moissette did the adsorption experiments in the solid-state, this fact may have led to differences in the adsorption behavior.

## 2.2 N, N, N', N' -tetramethyl-p-phenylenediamine (TMPD) and N, N, N', N' -tetramethylbenzidine (TMB)

N, N, N', N' -tetramethyl-p-phenylenediamine (TMPD) and N, N, N', N' -tetramethylbenzidine (TMB) were used as probes to characterize the nature of active sites in acid zeolite HZSM-5 [12]. These two amines are strong electron donors and are known to have low ionization potentials in the gas phase and to exhibit proton affinity. The rod-shaped N, N, N', N' - tetramethyl-p-phenylenediamine (TMPD) and N, N, N', N' - tetramethylbenzidine (TMB) molecules can penetrate within the porous void of ZSM-5 zeolites.

After several days of the mixing of TMPD and HZSM-5 powders, an intense UV-visible spectrum with the vibronic structure of  $\text{TMPD}^{*+}$  between 500 and 650 nm is observed. The vibrational progression of the  $\text{TMPD}^{*+}$  band (with peaks separated by  $\sim 1500\text{ cm}^{-1}$ ) is assigned to the stretching mode of the aromatic ring. RR and off-resonance Raman spectra of the mixed TMPD and HZSM-5 powders were obtained with 514.4 and 632.0 nm excitation and 1064 nm, respectively. All the spectra are very similar, with wavenumbers and intensities characteristic of the  $\text{TMPD}^{*+}$  species in solution. Raman bands assignable to neutral TMPD or protonated  $\text{H}_2\text{TMPD}$  are absent, which provided evidence of complete ionization of TMPD upon sorption in the experimental conditions.

Exposure of HZSM-5 to TMB for several days led to an intense absorption around 465 and 900 nm with the vibronic structure of  $\text{TMB}^{*+}$  between 400 and 500 nm. After several weeks a shoulder around 500 nm is induced in the spectra. This last feature was previously assigned to the  $\text{TMB}^{2+}$  dication [13]. Raman spectra of TMB adsorbed on HZSM-5 after several days of exposure were obtained with excitation at 514.5, 488.9, and 1064 nm. Exciting at 5145 nm within the electronic absorption of  $\text{TMB}^{2+}$  the resonance Raman spectrum of the dication is observed predominantly, compared with the bands of the  $\text{TMB}^{2+}$  in solution as charge-transfer bromide salt. The Raman spectrum obtained with 4880 nm excitation shows the simultaneous presence of  $\text{TMB}^{*+}$  and  $\text{TMB}^{2+}$  in the porous void of the zeolite. However, it is not possible to give a quantitative estimation of the amount of dication. Nonetheless, the dication is probably a minor species as the FT-Raman spectrum displays only the radical cation. It should be noted that  $\text{TMB}^{2+}$  decomposes quickly in neutral organic solutions, but it can be stabilized in acid solution. The acidic property of HZSM-5 appears suitable to stabilize the dication. After 15 days of interaction between TMB and the zeolite the absence of a Raman band assignable to neutral TMB or protonated  $\text{H}_2\text{TMB}$  provided evidence of complete ionization of TMB upon sorption under the experimental conditions.

## 2.3 Phenothiazine

Phenothiazines represent an important class of bioactive molecules. The photochemistry of phenothiazine (PTZ) (**Figure 1**) and its derivatives have been

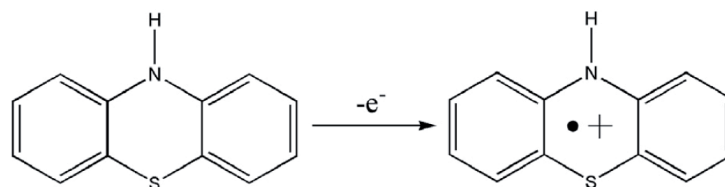


**Figure 1.**  
 Phenothiazine and its radical cation  $PTZ^{\bullet+}$ .

extensively studied because of its pharmacological interest [14]. Due to the low oxidation potential of PTZ, it is proposed that its role is to donate electrons or to transfer charge to the drug's receptor sites. This idea was corroborated by the discovery of many phenothiazine charge-transfer complexes. There has been an extensive study of the formation and reactivity of PTZ's stable radical cations [15], which are involved in an alternative to the biological activity mechanism [16].

As reported by Hester et al., the most intense electronic transition of PTZ radical cation ( $PTZ^{\bullet+}$ ) in the visible region can be found at 513 nm [17]. A resonance Raman investigation of  $PTZ^{\bullet+}$  in an aqueous solution was carried out by the authors, following the contour of the band. An enhancement was observed in several Raman bands, with the most intensified one being the one at  $476\text{ cm}^{-1}$ . This band was tentatively assigned to a CNC angular deformation mode. A band at  $644\text{ cm}^{-1}$ , assigned to the C-N stretching mode was also enhanced. Both bands have frequencies shifted to higher values compared to the ground state of the parent compounds which led them to suggest that the electron density in the radical cation of phenothiazine is localized on the N atom.

An RRS of  $PTZ^{\bullet+}$  obtained from the interaction of the neutral molecules with the mordenite zeolite, which has strong oxidizing sites was performed [18]. Phenothiazine is adsorbed in larger amounts in the acid sites of mordenite due to its larger pores. The observation of a pink color soon after PTZ was adsorbed on the mordenite is indicative of the formation of the radical cation  $PTZ^{\bullet+}$ . **Figure 2** shows the strongest band in the PTZ visible spectrum, located at 516 nm, which was attributed by Hester et al. to the radical cation  $PTZ^{\bullet+}$  [17]. The electronic spectrum calculated by the TDDFT method for  $PTZ^{\bullet+}$  is also displayed (**Figure 3**).

The RR spectra were excited with laser lines close to the most intense electronic transition of  $PTZ^{\bullet+}$  located at 516 nm.

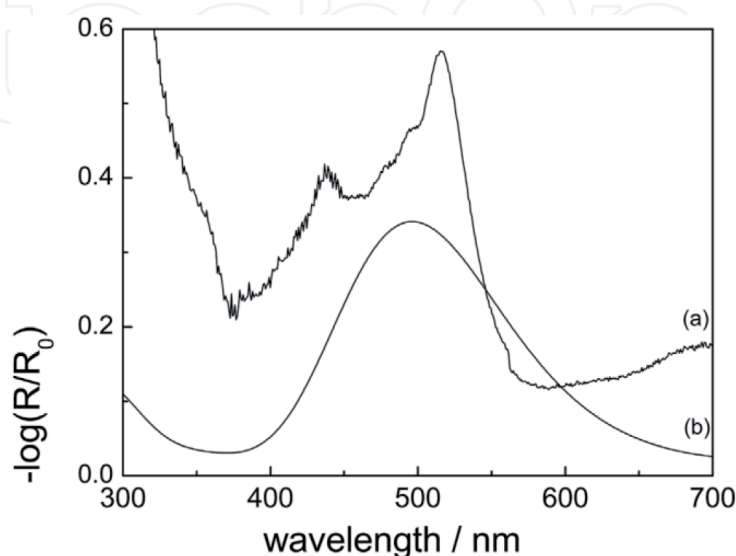


**Figure 2.**  
 (a) Diffuse reflectance spectrum of PTZ adsorbed on mordenite; (b) TDDFT (time-dependent density functional theory) calculated electronic spectrum of  $PTZ^{\bullet+}$  [18].

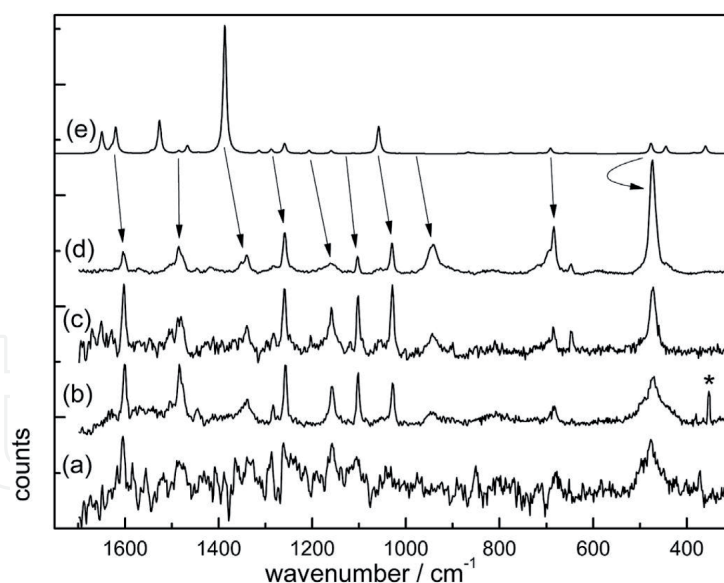


**Figure 3.**

RR spectra of PTZ adsorbed on mordenite zeolite at the exciting wavelengths: a) 457.9 nm; b) 488.0 nm; c) 496.5 nm; d) 514.5 nm; e) calculated. Arrows indicate the corresponding bands. Asterisk indicates a plasma line [18].

Exciting with 457.9 nm radiation gives rise to the weakest Raman spectrum. Raman excitation with radiations near 514.5 nm (488.0 and 496.5 nm).

It was noticed that excitation with 457.9 nm radiation gave the weaker Raman signal, while other wavelengths led to the increase of the Raman signal, with characteristic  $\text{PTZ}^{\bullet+}$  Raman bands showing up. Raman spectra excited near 514.5 nm (488.0 and 496.5 nm) also show enhancement of several vibrational modes, involving ring, CNC, and CSC vibrations, while with excitation at 514.5 nm there is a striking difference, giving the highest RR intensity and the best signal/noise ratio together with significative enhancement of the band at  $476\text{ cm}^{-1}$ . This fact can be explained by the resonance with the electronic transition band at ca. 516 nm.

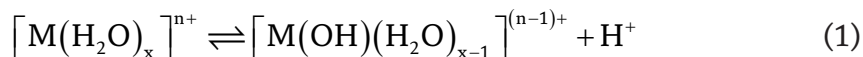
The most intensified Raman band at  $476\text{ cm}^{-1}$  was assigned to a CSC bending mode, according to DFT (density functional theory) B3LYP/6-31G(d,p) and TDDFT (time-dependent DFT) calculations, distinct from the previous assignment of Hester et al. Luchez et al. [19] also have obtained the  $\text{PTZ}^{\bullet+}$  radicals in mordenite, HZSM-5, and H-FER zeolites, following the reaction by UV-visible and Raman spectra. Two wavelengths, 1064 nm and 6328 nm, were used to excite the Raman spectra, but none of them reached the energy of the main electronic transition of  $\text{PTZ}^{\bullet+}$ , so in this condition, it is not possible to obtain the RR spectrum of this species.

### 3. Clays

Clay minerals are aluminosilicates, most of them of layered structures with tetrahedral silicate and octahedral aluminate sheets. The tetrahedral cation,  $\text{Si}^{4+}$ , can be replaced by  $\text{Al}^{3+}$  or  $\text{Fe}^{3+}$  cations, and the octahedral cations normally are  $\text{Al}^{3+}$ ,  $\text{Mg}^{2+}$ ,  $\text{Fe}^{2+}$ , and  $\text{Fe}^{3+}$  [20].

Smectite clays, (which have been most often used in organic reactions), have a 2:1 layer type, where one octahedral sheet is sandwiched by two tetrahedral sheets. If in the 2:1 layer-type aluminosilicate, the  $\text{Al}^{3+}$  is substituted by divalent cations, as  $\text{Mg}^{2+}$  (montmorillonite) in an octahedral sheet, results in a negative charge [21]. To balance the layer charge, cations are introduced between the layers. These cations are hydrated and exchangeable. In natural clays they are typically  $\text{Na}^+$ ,  $\text{K}^+$ ,  $\text{Ca}^{2+}$ , and  $\text{Mg}^{2+}$ ; similar ions can be exchanged with these ions. Smectite clays have the unique properties of

cation exchange capacity, intercalation, and swelling ability, which are important factors in their activity for various reactions involving organic molecules. Clays dried to low water content can behave as acids [22, 23]. Cation-exchanged montmorillonites act as strong Brönsted acids, where the reactive protons are derived from the dissociation of hydrated water molecules because of polarization by exchangeable cations. This situation may be represented by the following equilibrium reaction (Eq. 1):



Equilibrium reaction between  $[M(H_2O)_x]^{n+}$  and the respective species following dissociation of hydrated water molecule and  $H^+$ .

Brönsted acidity results from the terminal hydroxy groups on the external surface and the hydrated cations in the space between the layers of the clay. Lewis acidity is due to central metal ions such as  $Al^{3+}$ ,  $Mg^{2+}$ , and  $Fe^{3+}$  in the lattice and also from other metallic cations in the interlamellar space. Often the central metal ions are fully bonded to adjacent oxygen atoms in an octahedral site; so, these intact octahedra within the crystal arrays are unable of originating much Lewis acidity. Nevertheless, in the case of zeolites with small particle size, for instance, MMT K10 (typically 5–10  $\mu m$ ), what happens is that the sandwich layers are squashed to a remarkable extent, generating many broken edges of stacked layers, which contribute to Brönsted as well as Lewis acidity

The Lewis acid sites interaction between the metal cation and adsorbed organic molecules, especially with electron-donating character, results in electron transfer from the organic molecule to metal cation [24] with the consequent formation of radical cations and the reduction of metal ions to lower valency.

Mortland and Pinnavaia reported the interaction of some aromatic organic molecules with transition metal ions ( $Cu^{2+}$ ,  $Fe^{3+}$ ) exchanged montmorillonite. They observed the formation of colored adsorption complexes, which was explained due to the electron transfer from the aromatic molecule to the metal ion [25, 26].

The formation of aromatic radical cations was also observed by Pinnavaia et al. upon the adsorption of aromatic molecules on  $Cu^{2+}$ ,  $Fe^{3+}$  and  $VO^{2+}$  cation exchanged layered silicates (hectorite). Electron spin resonance spectra were useful to identify the radical cations while UV absorption spectra showed the presence of two species. Besides the radical cation, a charge transfer complex between the metal cation and the aromatic molecule was also observed. Infrared spectra of the adsorbed samples also showed that after some days oligomers and polymers of benzene, toluene, and anisole were formed [27].

### 3.1 p-dimethoxy benzene

Y. Soma, M. Soma, and I. Harada investigated the interaction of several aromatic molecules with clays, mainly transition metal exchanged montmorillonites using Raman spectroscopy in order to characterize the chromophore responsible for the absorption in the UV–visible region. P-dimethoxy benzene was the first one chosen by the authors [28] because the RR spectra of the radical cation of this molecule in solution had already been investigated by Ernstbrunner et al. [29]. The Raman spectra of p-dimethoxy benzene adsorbed on  $Cu^{2+}$ - and  $Ru^{3+}$ - montmorillonite were similar to the respective spectrum of p-dimethoxy benzene radical cation reported by Ernstbrunner et al. for the species in solution. RR enhancement in the blue region (maximum with excitation at 457.9 nm) was observed in agreement with the absorption band maxima at 435 and 450 nm. The most intensified band was the ring stretching at  $1622\text{ cm}^{-1}$ . It is also noticeable that the ring breathing band at  $820\text{ cm}^{-1}$  which is the strongest band in the neutral molecule, is very weak in the cation. The



enhancement of the ring stretching mode and the weakness of the ring breathing mode are also observed in the adsorbed samples on  $\text{Cu}^{2+}$ - and  $\text{Ru}^{3+}$ -montmorillonite.

### 3.2 Anisole

When anisole is adsorbed on  $\text{Cu(II)}$ -montmorillonite, the interaction between the adsorbate and the clay gives rise to several species, depending on the presence of water [30]. In a dry atmosphere, the sample has a green-blue color. In the UV visible spectrum, a broadband from  $\sim 550$  nm to  $\sim 850$  nm and other bands with the maximum at ca. 470 nm are observed. The RR spectra with excitation wavelengths of 6100 nm and 4570 nm are shown in **Figure 4(b)** and **(c)**, respectively, along with the Raman spectrum of liquid anisole. The RR spectrum excited with 6100 nm has bands at 995, 1208, 1325, 1528, and 1618  $\text{cm}^{-1}$ , that resembles the spectrum of 4,4'-dimethoxybiphenyl but the inter ring CC stretching at 1325  $\text{cm}^{-1}$  is upshifted, indicating the formation of a radical cation species of this molecule, similar to observed in the spectrum of 4,4'-dimethoxybiphenyl on  $\text{Cu}^{2+}$ - and  $\text{Ru}^{3+}$ -montmorillonite, reported in the same article [30]. Exciting with 457.9 nm a more complex spectrum is observed, as can be seen in **Figure 4(c)**. The authors made a deconvolution of the spectrum, which allowed the distinction of two spectra, the one in black is similar to the spectrum observed with 610.0 nm excitation, due to 4,4'-dimethoxybiphenyl radical cation, and the other in white has a resemblance with the spectrum of liquid anisole, but with shifts in some bands, as the ring breathing mode (925  $\text{cm}^{-1}$  compared to 995  $\text{cm}^{-1}$  in the liquid anisole spectrum). Another difference is the intensification of the ring stretching band at around 1600  $\text{cm}^{-1}$ , which is a signal of radical cation formation.

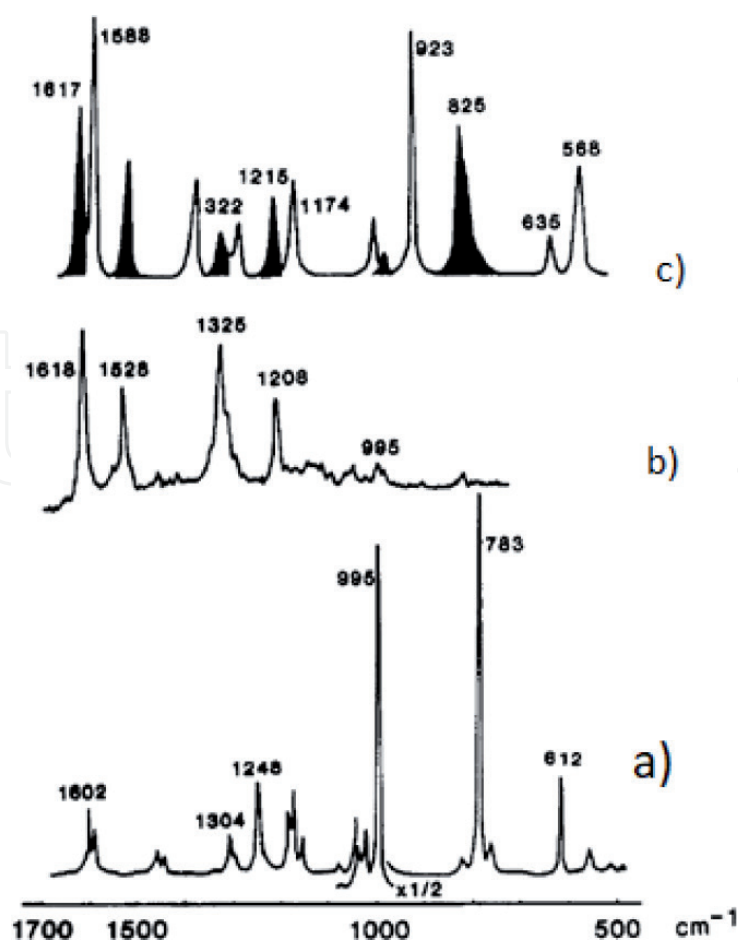


**Figure 4.**

(a) Raman spectrum of liquid anisole with 524.5 nm exciting wavelength and RR spectra of anisole adsorbed on  $\text{Cu(II)}$ -montmorillonite with (b) 610.0 nm and (c) 457.9 nm exciting wavelengths. Adapted from Soma et al. [30].

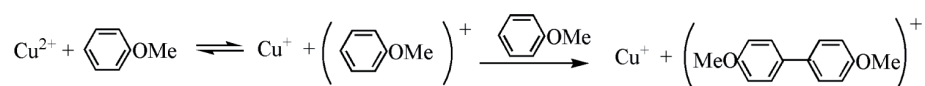


**Figure 5.**

Reactions occurring with anisole in Cu (II)-montmorillonite. Adapted from [30].

The authors proposed the following reactions to take place with anisole in the interlayer of the Cu(II)-montmorillonite (**Figure 5**).

The first reaction, a redox reaction forming  $\text{Cu}^+$  and the radical cation of anisole is favored in a dry atmosphere. In the second one anisole, radical cation reacts with neutral anisole, forming 4,4'-dimethoxybiphenyl radical cation.

### 3.3 Benzene

Soma et al. studied benzene adsorbed on  $\text{Cu}^{2+}$ -montmorillonite by RR spectroscopy [31]. Two species were observed: type II (red form), formed upon adsorption in an exhaustively dried atmosphere, and type I (yellow form) when exposed to humid air. Type I has a band with an absorption maximum at 380 nm while type II has an absorption maximum at 520 nm, besides a strong broad absorption that begins at 800 nm and extends into the near-infrared region.

The RR spectra of benzene adsorbed on  $\text{Cu}^{2+}$ -montmorillonite with excitation at 4579 and 5145 nm are very different from the Raman spectra of liquid benzene, resembling the spectra of p-phenylene molecules, e.g. p-terphenyl or p-quaterphenyl, indicating that oligomerization occurred on the clay surface. The presence of the inter ring C-C stretching at  $1324\text{ cm}^{-1}$  (type II) or  $1240\text{ cm}^{-1}$  (type I) is strong evidence of oligomerization. Type I and Type II are assigned to poly p-phenylene and poly p-phenylene radical cation, respectively, based on the results of RR spectra of poly p-phenylene (PPP) and  $\text{AsF}_5$ -PPP complex reported by Tzinis [32]. He observed a shift to a higher frequency of the inter ring C-C stretching in the complex compared to the bulk PPP. Based on the results of RR spectra and absorption spectra, it was concluded that benzene adsorbed on  $\text{Cu}^{2+}$ -montmorillonite is polymerized to PPP cation (type II) and reversibly reduced to PPP in humid air (type I) as follows (**Figure 6**).

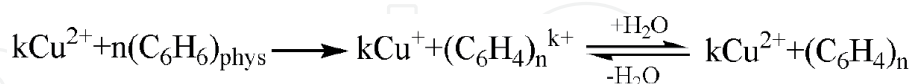


**Figure 6.**

Reactions of benzene with Cu(II)-montmorillonite. Adapted from [31].

$(\text{C}_6\text{H}_6)_{\text{phys}}$  means physically adsorbed benzene,  $(\text{C}_6\text{H}_4)_n$  and  $(\text{C}_6\text{H}_4)_n^{k+}$ , PPP and its cation, respectively.

Benzene adsorbed on  $\text{Fe}^{3+}$ - and  $\text{Ru}^{3+}$ -montmorillonite was also investigated by RR spectroscopy and showed a similar behavior; two species being formed, type I in humid air and type II in the dry atmosphere [33]. The authors noted, however, a difference between benzene/ $\text{Fe}^{3+}$ - and benzene/ $\text{Cu}^{2+}$ -montmorillonite: for the first one the transformation of type II to type I in humid air did not occur easily mainly after repeating the reaction, in contrast to what was observed with  $\text{Cu}^{2+}$ -montmorillonite complex.

### 3.4 Benzidine

Aqueous suspensions of benzidine and montmorillonite clay (BZ-MMT system) give rise to samples with blue, yellow, purple, and orange-brown colors, depending

on the pH of the suspension. In order to assign the species formed in these samples, in situ RR spectroscopy investigation was performed [34].

From pH 3 to 9, the main species responsible for the blue color is the radical cation of BZ ( $\text{BZ}^{\cdot+}$ ) which has  $\lambda(\text{max})$  at 600 nm. At pH lower than 3, the major species that gives rise to the yellow color is the dication,  $\text{BZ}^{2+}$  with  $\lambda(\text{max})$  at 440 nm. Following the dehydration of the blue BZ-MMT slurry, a yellow color appears, which was assigned to  $\text{BZ}^{\cdot+}$  and  $\text{BZ}^{2+}$  species, according to its RR spectrum. At pH higher than 9, the orange-brown colored sample was characterized as poly(benzidine) (PBZ). When the blue BZ-MMT aqueous suspension was left standing for 3 weeks a purple color appeared and it was found to be from a mixture of  $\text{BZ}^{\cdot+}$  and  $\text{BZ}^{2+}$  species together with PBZ. Synthetic Syn1 and pillared MMT clays in aqueous suspensions at different pHs were also tested to investigate the possibility of BZ oxidation. In these acidic clays, only the  $\text{BZ}^{\cdot+}$  was identified,  $\text{BZ}^{2+}$  species was not observed probably due to the majority presence of the less reactive  $\text{BZ}^{\cdot+}$ . At pHs above 9, the benzidine polymerization through the reaction between unprotonated  $\text{BZ}^{\cdot+}$  radical cations is catalyzed by the clay.

#### 4. Sulfated metal oxides

The preparation and the highly acid properties of sulfated metal oxide were reported for the first time by Hino and Arata [35] and Hino et al. [36], who investigated the catalytic properties of sulfated  $\text{TiO}_2$  and  $\text{ZrO}_2$ . These metal oxides were able to catalyze the isomerization of n-butane at room temperature, which only very strong acid catalysts are able to do. Thereafter they have been considered by some authors as superacids. In sulfated metal oxides, there are Lewis acid sites and Brönsted acid sites. The super acidity of these materials is attributed to the Brönsted and Lewis acid sites that have increased acidity due to the inductive effect of sulfate, which is coordinately bound to the  $\text{Ti}^{4+}$ . The sulfate group act as an electron-withdrawing group, making  $\text{Ti}^{4+}$  more electron-deficient, that is, a strong Lewis acid site, which in turn also withdraws electron density from the -OH group, creating or increasing the Brönsted acid site, as can be seen in **Figure 7**.

The unusual catalytic properties of these materials are attributed to the presence of very strong Lewis or Brönsted acid sites or both types of sites or to their oxidative ability. The oxidative ability was postulated by Ghenciu and Farcasiu [38], who observed that benzene was oxidized when adsorbed on sulfated  $\text{ZrO}_2$  and heated at 373 K. Several oxidation products, such as phenyl esters and phenols were formed, which were evidence of the presence of oxidizing sites [38].

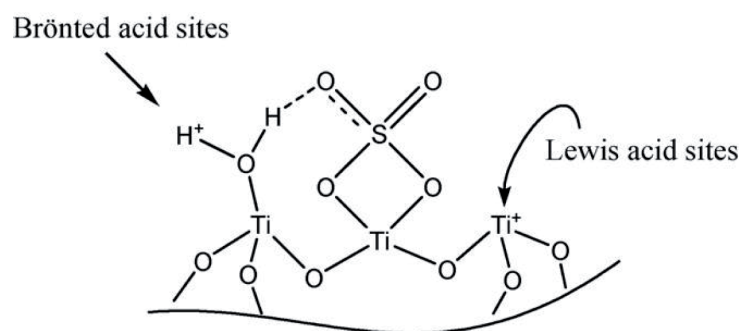


**Figure 7.**

*Illustrative structure of sulfated titania, representing the sulfate linked to the metal on the chelate form and indicating the Lewis and Brönsted acid sites. [37].*

The strong ionizing properties of sulfated  $\text{ZrO}_2$  and its relation to the catalytic activity were investigated by Chen et al. [39]. Benzene was used as a probe to study to evaluate the strong ionizing properties of sulfated  $\text{ZrO}_2$  due to its high ionizing potential value (9.24 eV). In the ESR spectrum, a hyperfine structured peak was observed and attributed to a biphenyl cation. They proposed the following explanation: a two-step process took place as a consequence of the interaction of benzene with sulfated  $\text{ZrO}_2$ . A CT complex between sulfated  $\text{ZrO}_2$  and benzene was formed in the first step. Then a complete electron transfer from benzene to the  $\text{ZrO}_2$  occurred, originating a benzene radical cation, this, in turn, reacted with a benzene molecule, forming the biphenyl radical cation.

As with sulfated  $\text{ZrO}_2$ , sulfated  $\text{TiO}_2$  (a solid acid) also may have the ability to interact with aromatic compounds and form CT complexes and may oxidize aromatic molecules with the formation of radical cations.

#### 4.1 Benzene

A RR spectroscopy study using a commercial sulfated  $\text{TiO}_2$ , following its interaction with benzene was reported by our group [40]. Besides the remarkable enhancement of  $\nu(\text{CC})$  ring modes, the appearance of non-totally symmetric vibrations was observed in the Raman spectra. The presence of benzene was confirmed by the characteristic benzene ring breathing mode. The preferential enhancement of the  $\nu(\text{CC})$  ring modes and the appearance of non-totally symmetric vibrations were explained by the RR enhancement due to benzene to  $\text{Ti}(\text{IV})$  CT transition [41]. Negligible amounts of radicals were detected in the ESR spectrum, because of the moderate strength of the acid sites of the sulfated  $\text{TiO}_2$  used in the study. The RR spectra of benzene on sulfated  $\text{TiO}_2$  with 457.9 and 476.5 nm exciting wavelengths are shown in **Figure 8**. The bands of anatase  $\text{TiO}_2$  (marked with asterisks) acts as an internal standard to measure the Raman signal intensification. It is noteworthy the striking enhancement of the band at ca.  $1600\text{ cm}^{-1}$ , due to benzene ring CC stretching mode exciting with 476.5 nm. This wavelength corresponds to an absorption band in this energy range, assigned to a charge transfer transition. This sulfated  $\text{TiO}_2$  was not able to oxidize benzene, a molecule with relatively high ionization potential, but a strong interaction occurred, as can be seen in the RR spectra.

The experimental Raman spectrum of the benzene radical cation is unknown. However, the Raman spectra of the phenylene oligomeric radical cations such as biphenyl [42] and p-terphenyl that are formed after adsorption on zeolites [43]

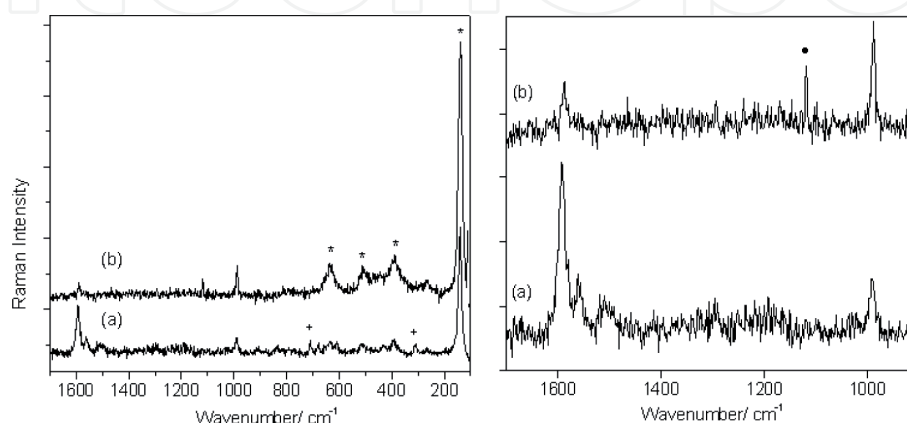


**Figure 8.** RR spectra of benzene on sulfated  $\text{TiO}_2$  with two exciting wavelengths: (a) 457.9 nm and (b) 476.5 nm. On the left: The 100–1700  $\text{cm}^{-1}$  spectral region and on the right: The 900–1700  $\text{cm}^{-1}$  region.  $\text{TiO}_2$  bands, +plasma lines of the 457.9 argon-ion laser, Hg lamp line.



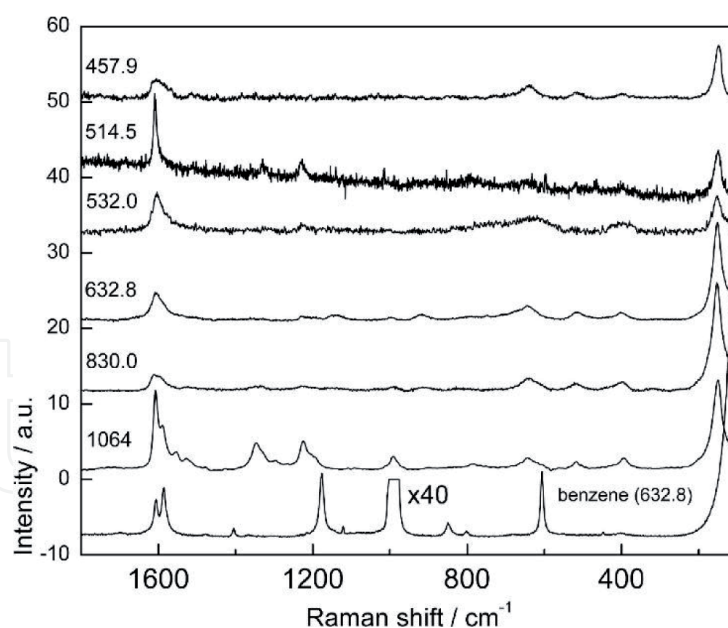


**Figure 9.**

RR spectra of benzene/sulfated  $\text{TiO}_2^*$  sample and liquid benzene at the indicated exciting wavelengths [45].

\* = sulfated  $\text{TiO}_2$  prepared by sol-gel method.

have been reported in the literature. These species present the RR effect as reported in the literature for some radical cations.

We have performed an investigation of benzene adsorbed on a very highly acid sulfated  $\text{TiO}_2$ , synthesized by sol-gel method [44] at room temperature. A tentative assignment of the species formed from the interaction was done with Raman and electron spin resonance (ESR) spectroscopy [45]. From the absorption spectra in the visible and near-infrared (NIR), it was possible to identify these species as phenylene oligomer radical cations. The UV-visible-near IR spectrum of benzene/sulfated  $\text{TiO}_2$  sample shows two maxima, one between 400 and 500 nm and the other in the NIR region that begins at ca. 1100 nm and increases towards the infrared. An explanation to this spectrum is based on the RR spectroscopy study of the interaction of benzene with Fe(III)-doped montmorillonite, reported by Soma et al. [31]. They observed two kinds of spectra. The dried sample had an absorption band at 510 nm and was named Type I. When moisture was allowed to contact the dried sample, the band at 510 nm shifted to 380 nm and the spectrum was named Type II. Both types have an absorption that begins at 660 nm and extends to the NIR region. Type I and Type II are assigned to PPP and PPP radical cation, respectively. The Raman spectra of benzene with sulfated  $\text{TiO}_2$ , excited with several excitation wavelengths are seen in **Figure 9**. It is evident that the spectra do not resemble the spectrum of liquid benzene, mainly because of the absence of the ring breathing mode at  $998\text{ cm}^{-1}$ , the most intense band of neat benzene. It is noteworthy the intensification of some bands, notably the one at ca.  $1600\text{ cm}^{-1}$ , with the maximum of intensification using exciting wavelengths of 514.5 nm and 1064 nm. These two wavelengths correspond to the two absorptions in the visible-near IR regions of the benzene/sulfated  $\text{TiO}_2$  sample. The behavior is similar to that observed by Soma et al. RR spectra were observed and the species that gave rise to these spectra are phenylene oligomers or phenylene oligomer radical cations.

## 5. Conclusions

Several examples of the use of RR spectroscopy as a tool to identify species formed from the interaction of solid acids with several aromatic molecules were presented. The solid acids have strong acid sites, which can oxidize molecules

adsorbed on them or originate charge-transfer complexes. The solid acids were zeolites, clays, and sulfated metal oxides, because of their strong acid sites. Selected works from the literature that report spontaneous ionization of molecules adsorbed on the solid acids and the follow-up of the intermediate species by RR spectroscopy were reported. The intermediate species are radical cations or charge transfer complexes that have absorptions in the visible and in some cases near the IR region. The RR spectra were able to characterize the intermediate species and also to provide information of the chromophore responsible for the electronic transition, because of the preferential RR enhancement of its vibrational modes.

## Acknowledgements


The author is grateful to Molecular Spectroscopy Laboratory (Institute of Chemistry, São Paulo University, São Paulo) for the Raman spectra on Jobin-Yvon U-1000 spectrometer and to FAPESP (process 2017/06194-2) for the financial support.

## Author details

Lucia Kiyomi Noda  
Federal University of São Paulo, Diadema, Brazil

\*Address all correspondence to: [lucia.noda@unifesp.br](mailto:lucia.noda@unifesp.br)

## IntechOpen

© 2021 The Author(s). Licensee IntechOpen. This chapter is distributed under the terms of the Creative Commons Attribution License (<http://creativecommons.org/licenses/by/3.0>), which permits unrestricted use, distribution, and reproduction in any medium, provided the original work is properly cited. 

## References

- [1] Hendra PJ, Passingham G, Warnes GM, Burch R, Rawlence DJ. Fourier transform Raman spectroscopy in the study of species adsorbed on catalyst surfaces. *Chemical Physics Letters*. 1989;**164**(2,3):178-184. DOI: 10.1016/0009-2614(89)85012-2
- [2] Hess H. New advances in using Raman spectroscopy for the characterization of catalysts and catalytic reactions. *Chemical Society Reviews*. 2021;**50**:3519-3564. DOI: 10.1039/d0cs01059f
- [3] Clark RJH, Dines TJ. Resonance raman spectroscopy, and its application to inorganic chemistry. *Angewandte Chemie, International Edition*. 1986;**25**(2):131-158. DOI: 10.1002/anie.198601311. ISSN 0570-0833
- [4] Ramamurthy V, Caspar JV, Corbin DR. Modification of photochemical reactivity by zeolites – generation, entrapment and spectroscopic characterization of radical cations of alpha-omega-diphenyl polyenes within the channels of pentasil zeolites. *Journal of the American Chemical Society*. 1991;**113**:594-600. DOI: 10.1021/ja00002a030
- [5] Moissette A, Lobo RF, Vezin H, Al-Majnouni KA, Brémard C. Long Lived Charge Separated States Induced by trans-Stilbene Incorporation in the Pores of Brønsted Acidic HZSM-5 Zeolites: Effect of Gallium on the Spontaneous Ionization Process. *Journal of Physical Chemistry C*. 2010;**114**:10280-10290. DOI: 10.1021/jp103838b
- [6] Werst DW, Trifunac AD. Observation of radical cations of by swiftness or by stealth. *Accounts of Chemical Research*. 1998;**31**:651-657. DOI: 10.1021/ar970234w
- [7] Garcia H, Roth HD. Generation and reactions of organic radical cations in zeolites. *Chemical Reviews*. 2002;**102**(11):3947-4008. DOI: 10.1021/cr980026x
- [8] Hureau M, Moissette A, Smirnov KS, Jobic H. Combined spectroscopic and modeling study of trans-stilbene molecule in cation-exchanged zsm-5 zeolites. *Journal of Physical Chemistry C*. 2012;**116**:15510-15518. DOI: 10.1021/jp305631q
- [9] Vezin H, Moissette A, Hureau M, Brémard C. Trans-stilbene incorporation in acidic medium-pore ZSM-5 zeolite: A pulsed EPR study. *ChemPhysChem*. 2006;**7**:2474-2477. DOI: 10.1002/cphc.200600279
- [10] Moissette A, Hureau M, Moreau M, Cornard JP. Pore selectivity and electron transfers in HZSM-5 single crystals: A Raman microspectroscopy mapping and confocal fluorescence imaging combined study. *Physical Chemistry Chemical Physics*. 2020;**22**:12745-12756. DOI: 10.1039/d0cp02018d
- [11] Moissette A, Brémard C, Hureau M, Vezin H. Slow interfacial electron hole transfer of a trans-stilbene radical cation photoinduced in a channel of nonacidic aluminum rich ZSM-5 zeolite. *Journal of Physical Chemistry C*. 2007;**111**:2310-2317. DOI: 10.1021/jp066216q
- [12] Moissette A, Gener I, Brémard C. Probing the spontaneous ionization of aromatic amines by adsorption in activated acidic zeolite HZSM-5. *Journal of Raman Spectroscopy*. 2002;**33**:381-389. DOI: 10.1002/jrs.836
- [13] Guichard V, Bourkba A, Poizat O, Buntinx G. Vibrational studies of reactive intermediates of aromatic amines. 2. Free-radical cation and dication resonance Raman spectroscopy of N, N, N', N'-tetramethylbenzidine and N, N, N', N'-tetramethylbenzidine. *The Journal of Physical Chemistry*.

1989;**93**:4429-4435. DOI: 10.1021/j100348a012

[14] Jaszczyszyn A, Gasiorowski K, Swiatek P, Malinka W, Ciezlik-Boczula K, Petrus JB, et al. Chemical structure of phenothiazines and their biological activity. *Pharmacological Reports*. 2012;**64**(1):16-23. DOI: 10.1016/S1734-1140(12)70726-0

[15] Turro NJ, Khudyakov IV, Van Willigen H. Photoionization of phenothiazine: EPR detection of reactions of the polarized solvated electron. *Journal of the American Chemical Society*. 1995;**117**(49): 12273-12280. DOI: 10.1021/ja00154a029

[16] Philips DL, Pan D. Raman and density functional study of the  $S_0$  state of phenothiazine and the radical cation of phenothiazine. *The Journal of Physical Chemistry. A*. 1999;**103**(24):4737-4743. DOI: 10.1021/jp990399h

[17] Hester RE, Williams KPJ. Free radical studies by resonance Raman spectroscopy: Phenothiazine, 10-methylphenothiazine and phenoxazine radical cations. *Journal of the Chemical Society, Perkin Transactions 2*. 1981;**77**:852-859. DOI: 10.1039/P29810000852

[18] Noda LK, Gonçalves NS. Assignment of the electronic transition of phenothiazine radical cation in the visible region - a resonance Raman spectroscopy and theoretical calculation investigation. *Journal of Molecular Structure*. 2019;**1191**:253-258. DOI: 10.1016/j.molstruc.2019.04.053

[19] Luchez F, Carre' S, Moissette A, Poizat O. Sorption and spontaneous ionization of phenothiazine within channel type zeolites: Effect of the confinement on the electron transfers. *RSC Advances*. 2011;**1**:341-350. DOI: 10.1039/c1ra00220a

[20] Soma Y, Soma M. Chemical reactions of organic compounds on clay surfaces. *Environmental Health Perspectives*. 1989;**83**:205-214. DOI: 10.2307/3430656

[21] Brindley GW, Brown G. *Crystal Structures of Clay Minerals and Their X-ray Identification*. London: Mineralogical Society of Great Britain; 1980. p. 518

[22] Laszlo P. Chemical reactions on clays. *Science*. 1987;**235**:1473-1477. DOI: 10.1126/science.235.4795.1473

[23] Pinnavaia TJ. Intercalated clay catalysts. *Science*. 1983;**220**:365-371. DOI: 10.1126/science.220.4595.365

[24] Theng BKG. Clay-activated organic reactions. In: *Developments in Sedimentology* (H. Van Olphen and F. Vanale, Eds.) vol. 35. Elsevier: Amsterdam; 1982. pp. 197-238

[25] Mortland MM, Pinnavaia TJ. Formation of copper(II) arene complexes on the interlamellar surfaces of montmorillonite. *Nature*. 1971;**229**:75-77. DOI: 10.1038/physci229075a0

[26] Pinnavaia TJ, Mortland MM. Interlamellar metal complexes on layer silicate. I. Copper(II)-arene complexes on montmorillonite. *The Journal of Physical Chemistry*. 1971;**75**:3957-3962. DOI: 10.1021/j100695a007

[27] Pinnavaia TJ, Hall PL, Cady SS, Mortland MM. Aromatic radical cation formation on the intracrystal surfaces of transition metal layer lattice silicates. *The Journal of Physical Chemistry*. 1974;**78**:994-999. DOI: 10.1021/j100603a010

[28] Soma Y, Soma M, Harada I. Raman spectroscopic evidence of formation of p-dimethoxybenzene cation on Cu- and Ru- montmorillonites. *Chemical Physics Letters*. 1983;**94**(5):475-478. DOI: 10.1016/0009-2614(83)85035-0



- [29] Ernstbrunner E, Girling RB, Grossman WEL, Hester RE. Free radical studies by resonance Raman spectroscopy. 1. 1,4-dimethoxybenzene radical cation. *Journal of the Chemical Society, Perkin Transactions 2*. 1978;**2**:177-184. DOI: 10.1039/p29780000177
- [30] Soma Y, Soma M, Harada I. Reactions of aromatic molecules in the interlayer of transition-metal ion exchanged montmorillonite studied by Resonance Raman Spectroscopy. 2. Monosubstituted benzenes and 4,4'-disubstituted biphenyls. *The Journal of Physical Chemistry*. 1985;**89**(5):738-742. DOI: 10.1021/j150658a021
- [31] Soma Y, Soma M. Resonance Raman spectra of benzene adsorbed on Cu<sup>2+</sup>-montmorillonite. Formation of poly(p-phenylene) cations in the interlayer of the clay mineral. *Chemical Physics Letters*. 1983;**99**(2):153-156. DOI: 10.1016/0009-2614(83)80549-1
- [32] Tzinis C-H, Baughman RH, Risen WM Jr. Raman Spectra of Highly Conducting Poly-p-phenylene Complexes. Office of Naval Research; 1980. Providence, Rhode Island: Technical Report No. TR-80-01
- [33] Soma Y, Soma M, Harada I. The reaction of aromatic molecules in the interlayer of transition-metal ion-exchanged montmorillonite studied by resonance Raman spectroscopy. 1. Benzene and *p*-Phenylenes. *The Journal of Physical Chemistry*. 1984;**88**:3034-3038. DOI: 10.1021/j150658a021
- [34] Nascimento GM, Barbosa PSM, Constantino VRL, Temperini MLA. Benzidine oxidation on cationic clay surfaces in aqueous suspension monitored by in situ resonance Raman spectroscopy. *Colloids and Surfaces A: Physicochemical and Engineering Aspects*. 2006;**289**:39-46. DOI: 10.1016/j.colsurfa.2006.04.005
- [35] Hino M, Arata K. Reactions of butane and isobutane catalysed by titanium oxide treated with sulphate ion. Solid superacid catalyst. *Journal of the Chemical Society, Chemical Communications*. 1979;**24**:1148-1149. DOI: 10.1039/C39790001148
- [36] Hino M, Kobayashi S, Arata K. Solid catalyst treated with anion. 2. Reactions of butane and isobutane catalyzed by zirconium oxide treated with sulfate ion. Solid superacid catalyst. *Journal of the American Chemical Society*. 1979;**101**:6439-6441. DOI: 10.1021/ja00515a051
- [37] Almeida RM, Noda LK, Gonçalves NS, Meneghetti SMP, Meneghetti MR. Transesterification reaction of vegetable oils, using superacid sulfated TiO<sub>2</sub>-base catalysts. *Applied Catalysis A*. 2008;**347**:100-105. DOI: 10.1016/j.apcata.2008.06.006
- [38] Ghenciu A, Farcasiu D. Oxidizing ability as the defining factor of reactivity of sulfated zirconia. *Chemical Communications*. 1996;**2**:169-170. DOI: 10.1039/CC9960000169
- [39] Chen FR, Coudurier G, Joly JF, Védrine JC. Superacid and catalytic properties of sulfated zirconia. *Journal of Catalysis*. 1993;**143**(2):616-626. DOI: 10.1006/jcat.1993.1304
- [40] Noda LK, Rosales R, Gonçalves NS, Sala O. Evidences for charge-transfer complex formation in the benzene adsorption on sulfated TiO<sub>2</sub> – a resonance Raman spectroscopy investigation. *Journal of Raman Spectroscopy*. 2008;**39**(3):415-420. DOI: 10.1002/jrs.1843
- [41] Gonçalves NS, Noda LK. Spectroscopic study of the charge-transfer complexes TiCl<sub>4</sub>/styrene and TiCl<sub>4</sub>/polystyrene. *Journal of Molecular Structure*. 2017;**1146**:750-754. DOI: 10.1016/j.molstruc.2017.06.029
- [42] Buntinx G, Poizat O. Triplet (T<sub>1</sub>) state and radical cation resonance

Raman investigation of biphenyl derivatives. *The Journal of Chemical Physics*. 1989;**91**:2153-2162.  
DOI: 10.1063/1.457023

[43] Belhadj F, Moissette A, Bernard C, Hureau M, Derriche Z. Effects of spatial constraints and Brönsted acid site locations on para-terphenyl ionization and charge transfer in zeolites. *ChemPhysChem*. 2011;**12**:1378-1388.  
DOI: 10.1002/cphc.201000825

[44] Noda LK, Almeida RM, Probst LFD, Gonçalves NS. Characterization of sulfated TiO<sub>2</sub> prepared by the sol-gel method and its catalytic activity in the n-hexane isomerization reaction. *Journal of Molecular Catalysis A*. 2005;**225**(1):39-46. DOI: 10.1016/j.molcata.2004.08.025

[45] Gonçalves NS, Rettori D, Silva GMG, Noda LK. Spectroscopic study of radical cation species formed on sulfated TiO<sub>2</sub> upon benzene adsorption. *Vibrational Spectroscopy*. 2018;**99**:80-85. DOI: 10.1016/j.vibspec.2018.08.012